

# On the Impact of Control Signaling in RIS-Empowered Wireless Communications

FABIO SAGGESE<sup>1</sup> (Member, IEEE), VICTOR CROISFELT<sup>1</sup> (Graduate Student Member, IEEE),  
RADOSŁAW KOTABA<sup>1</sup>, KYRIAKOS STYLIANOPOULOS<sup>2</sup> (Graduate Student Member, IEEE),  
GEORGE C. ALEXANDROPOULOS<sup>2</sup> (Senior Member, IEEE), AND PETAR POPOVSKI<sup>1</sup> (Fellow, IEEE)

<sup>1</sup>Department of Electronic Systems, Aalborg University, 9200 Aalborg, Denmark

<sup>2</sup>Department of Informatics and Telecommunications, National and Kapodistrian University of Athens, 15784 Athens, Greece

CORRESPONDING AUTHOR: F. SAGGESE (e-mail: fasa@es.aau.dk)

This work was supported in part by the Villum Investigator grant "WATER" from the Villum Foundation, Denmark, and in part by the EU H2020 RISE-6G Project under Grant 101017011.

**ABSTRACT** The research on Reconfigurable Intelligent Surfaces (RISs) has dominantly been focused on physical-layer aspects and analyses of the achievable adaptation of the wireless propagation environment. Compared to that, questions related to system-level integration of RISs have received less attention. We address this research gap by analyzing the control signaling operations needed to integrate the RIS as a new wireless infrastructure element. As the main contribution of the paper, we build a systematic procedure for evaluating the impact of control operations on communication performance along two dimensions: *i*) the rate selection for the data channel (multiplexing or diversity), and *ii*) the allocated bandwidth of the control channels (in-band and out-of-band). Specifically, the first dimension results in two generic transmission paradigms: one focuses on optimizing RIS setting according to the propagation environment, labeled as optimization based on channel estimation (OPT-CE); the other is based on sweeping through predefined RIS phase configurations, labeled as codebook-based beam sweeping (CB-BSW). We analyze the communication performance in multiple setups built along these two dimensions. While necessarily simplified, our analysis reveals the basic trade-offs in RIS-assisted communications and the associated control operations: CB-BSW is better suited for high mobility scenarios since its operation is not conditional on performing channel estimation within the coherence time; OPT-CE performs significantly better when the channel coherence time is sufficiently long, but it requires exchanging more control data, necessitating higher control reliability and profiting more from out-of-band control channel design. Our systematic procedure can be easily adapted to include more complex systems and transmission modes.

**INDEX TERMS** Reconfigurable intelligent surfaces, control channel, protocol design, performance analysis.

## I. INTRODUCTION

RECONFIGURABLE intelligent surfaces (RISs) constitute a promising technology for sixth generation (6G) wireless networks, which has received significant attention within the relevant research community in recent years [1]. The main underlying idea is to electronically tune the reflective properties of a reconfigurable intelligent surface (RIS) to manipulate the phase, amplitude, and polarization of the incident electromagnetic waves [2]. This creates a propagation environment that is, at least, partially

controllable [3]. RISs can be fabricated with classical antenna elements controlled through switching elements or, more advanced, with metamaterials having tunable electromagnetic properties [4]. In the 6G context, the RIS technology has been identified as one of the cost-effective solutions to address the increasing demand for higher data rates, reduced latency, and increased coverage. In particular, an RIS can improve the received signal strength and minimize interference by reflecting signals to intended receivers and away from non-intended ones; this leads to applications

aiming for increased communication security [5] and/or reduced electromagnetic field exposure [6]. RISs can also extend the coverage of wireless communication systems by reflecting the signals to areas that are difficult to reach using conventional means [7].

The dominant part of the literature concerning RIS-aided communication systems deals with physical-layer (PHY) challenges. Different hardware architectures and accurate channel modeling were among the main topics investigated to understand the potential benefits of employing RIS – see [8], [9] and the reference therein. Among others, recent studies have explored physics-based derivation of RIS-parametrized end-to-end channel models, incorporating causality, frequency selectivity, as well as any arising mutual coupling effects [10]. Consequently, several works have focused on the *channel state information (CSI) acquisition in the presence of RISs through the design of specific channel estimation (CE) methods*, either relying on the observed equivalent end-to-end channel from the base station (BS) to the user equipment (UE), when dealing with solely reflective RISs, e.g., [11], [12], [13], or directly estimating individual channels – BS-to-RIS and RIS-to-UE – by using simultaneous reflecting and sensing RISs [14]. The latter RIS design belongs to the attempts to minimize the CE overhead [15], which can be considerably large due to the expected high numbers of RIS elements [16] or hardware-induced non-linearities [8]. Many other papers have investigated the potential benefits of RIS-aided systems in terms of spectral and energy efficiencies by optimizing the parameters of the RIS' elements alone or jointly with the operations of the BS, based on the knowledge of the CSI (see, e.g., [17], [18], [19]). From an implementation point of view, strategies that combine CSI acquisition and optimization belong to what we refer to in this work as the *optimization based on channel estimation (OPT-CE)* paradigm: the network elements operate using a CE method (e.g., [11]) to enable a decision-maker to obtain the CSI, which is then exploited to optimize RIS and BS communication parameters according to a specific algorithm, which is typically computationally expensive (e.g., [18]). A different research direction bypasses explicit CE and relies on the *codebook-based beam sweeping (CB-BSW)* paradigm, denoted by this name in [20], but already employed in previous works for different scopes (e.g., in [21], [22], [23]). Accordingly, the RIS is scheduled to successively switch between reflecting configurations from a predefined codebook so that the end-to-end system can discover the most suitable configuration [20], [21], [22], [23]. The predefined codebook can be practically optimized for different purposes [24]; a suitable approach is to use hierarchical codebook structures [23], [25].

Within the existing research literature, the questions related to link/medium access control (MAC) protocol and system-level integration of RISs have received less attention than PHY topics. On this matter, some papers focused on developing grant-free random access protocols

exploiting RIS spatial diversity [26], [27], [28], while others designed user multiplexing schemes based on pre-coordination between network nodes [29], [30]. However, *the literature lacks a systematic treatment of the control signaling required to remotely manage the behavior of the RISs and the UEs*, which is often exerted by the BS upon well-defined control channels (CCs). The study of control procedures is central to integrate the RIS as a new type of network element within the existing wireless infrastructure.

## A. RELATED LITERATURE

An extensive part of the literature assumes that the control over an RIS-aided communication system is error-free and instantaneous. For example, in [27] and later [28], the authors presented a detailed protocol for random access aided by an RIS. It was showcased that, despite the physical overhead of switching its configurations, the RIS brings notable performance benefits, allowing more UEs to access the BS on average. Similarly, in [31], the effect of re-transmission protocols in RIS-aided systems in the case of erroneous transmission was studied, but the control impact was ignored. This is also a common assumption in works related to channel estimation, power optimization, and channel capacity characterization – see, e.g., [8], [32], and references therein. Other works did not even specify the required control information to be exchanged between the communication entities. For instance, one of the first works focusing on fast RIS programmability [33] presented a multi-stage OPT-CE protocol with ideal control. By tasking the RIS to dynamically illuminate the area where a UE is located, the authors of [22] introduced a downlink (DL) transmission protocol including RIS configuration optimization based on UE localization, and pilot-aided end-to-end CE. In [23], a fast near-field alignment scheme belonging to the CB-BSW paradigm was proposed for the RIS phase-shifts and the transceiver beamformer, relying on a variable-width hierarchical RIS phase configuration codebook. Recently, [20] discussed the overhead and challenges of integrating the RIS into the network, arguing that the reduced overhead offered by CB-BSW schemes benefits the overall system performance, but the control signaling needed for those schemes was not investigated.

Nevertheless, the need for control when integrating the RIS in the network has been known since early works [34]. To mitigate this necessity, recent works such as [15], [35], [36] focused on designing autonomous RIS operating without any explicit control: the RIS adapts to the environment by using a minimal amount of information that it can capture by listening to CCs shared with UEs and through its own sensing capabilities. However, the RIS needs to be equipped with simultaneously reflecting and sensing elements [15], increasing the cost and the complexity of the device. For solely-reflective RISs, the problem of explicit control has been considered in [32] as the *control and programming phase*. Inspired by the concept of software-defined radio (SDR), different works propose the use of a software

application to control the RIS behavior, motivating the terms software-defined metasurfaces or software-controllable surfaces [37]. In this regard, [38], and [39] consider the implementation of such control strategies. However, these works do not provide a generalization of the possible control designs, nor evaluate their impact on the communication performance of the system as a whole.

To the best of the authors' knowledge, the only work that consider the impact of a (portion of) the control operations is [40]. Its authors propose a solution for the optimization of the RIS and BS beamformers, accounting for the overhead generated by the CSI acquisition, and the subsequent feedback of the optimized configuration toward the RIS. However, [40] does not comprehensively analyze the required control signaling, neglecting the influence of the RIS to the control of the UE, and assuming perfect reliability of the CCs. In other works unrelated to RIS topics, the control plane design has been studied from an L3 or above perspective, investigating, *e.g.*, the performance of deploying specific control solutions for software-defined networking (SDN) [41], [42], [43]. From a PHY and MAC layers perspective, the control plane performance depends on the resources employed by the CCs, see [44] and the reference therein. In this regard, the literature lacks an analysis of different CC designs for RIS-aided networks.

Due to the existing literature, we are interested in studying how the system performance is impacted by the design of the CCs in terms of rate and reliability, as well as the overhead/trade-offs incurred by the control signaling procedures needed for the communication paradigm employed.

## B. SCOPE & AIM

This paper aims to introduce a systematic procedure to identify and quantify the impact of control signaling on the performance of RIS-enabled wireless communications. The number of actual control options is subject to a combinatorial explosion due to the system's large number of configurable parameters, such as frame size or feedback design. Obviously, we cannot address all these designs in a single work, but what we are striving for is to get a simple, yet generic, methodology to analyze the impact of control that captures the essential design trade-offs and can be expanded to analyze other, more elaborate, designs. For this reason, in this paper, we keep the complexity of the RIS-aided system model at the minimum, *focusing on investigating the interaction between the control and the data planes*. Considering a single-antenna BS and narrowband communications, we analyze the communication performance when control signaling occurs over the RIS-CC linking the BS to the RIS, and the UE-CC that links the BS to the UE through the RIS. At the end of the paper, we further discuss how to relax some of the assumptions made to generalize the proposed procedure. We build our systematic procedure along the two following dimensions.

The *first dimension* is shaped around the distinctions between traditional communication paradigms of

multiplexing and diversity [45]. In a *multiplexing-oriented transmission*, a key performance indicator (KPI) of interest – *e.g.*, data rate – is adapted to the actual channel conditions based on the CSI obtained via CE. However, CE generally needs complex control signaling, implying a high control overhead. In an RIS-aided system, multiplexing transmission occurs under the OPT-CE paradigm, in which, the RIS response is purposefully configured to, for example, maximize the signal-to-noise ratio (SNR) of the end-to-end channel, based on acquired CSI, and the transmission data rate is adapted to the resulting achievable rate. In a *diversity transmission* scenario, the KPI is pre-established, and the UE relies on the expectation that the propagation environment will accommodate it. However, if the propagation environment does not meet these expectations, it can lead to an outage event, resulting in transmission failure. In an RIS-aided system, diversity transmission can be realized following the CB-BSW paradigm: a KPI is predetermined, *e.g.*, a target SNR; the UE transmits while the BS commands the RIS to load a series of different configurations, hoping that at least one of them will support the target KPI.

The *second dimension* regards how the resources used by the CCs physically relate to the ones employed for the data channel (DC) used for data communication [44]. We study the following two options. First, an *out-of-band CC (OB-CC)* uses communication resources orthogonal to the ones used by the DC. More precisely, an OB-CC exerts control over the propagation environment but is not affected by this control. Second, an *in-band CC (IB-CC)* uses the same communication resources as the DC. This implies that the IB-CC reduces the available resources to transmit data, likely decreasing the performance of the overall system. Moreover, communication over an IB-CC might be influenced by the RIS configuration loaded.

## C. CONTRIBUTIONS

The main contributions of this paper are:

- We develop a systematic procedure to analyze and quantify the impact of control signaling on RIS-empowered wireless communications based on the definition of three general phases: *Signaling*, *Algorithmic*, and *Payload*, related to control information transmission, computation, and data transmission, respectively.
- The proposed methodology is applied to communication strategies belonging to the OPT-CE and CB-BSW paradigms, evaluating the impact of overhead and the errors brought by the Signaling and Algorithmic phases to the payload transmission through the definition of the minimum required control operations.
- Performance trade-offs are investigated through numerical simulations, testing against the DC coherence time, quantifying the impact of algorithmic errors, and evaluating the reliability of OB-CC and IB-CC designs.

Our analysis suggests that employing either OPT-CE or CB-BSW depends on the specific service requirements and

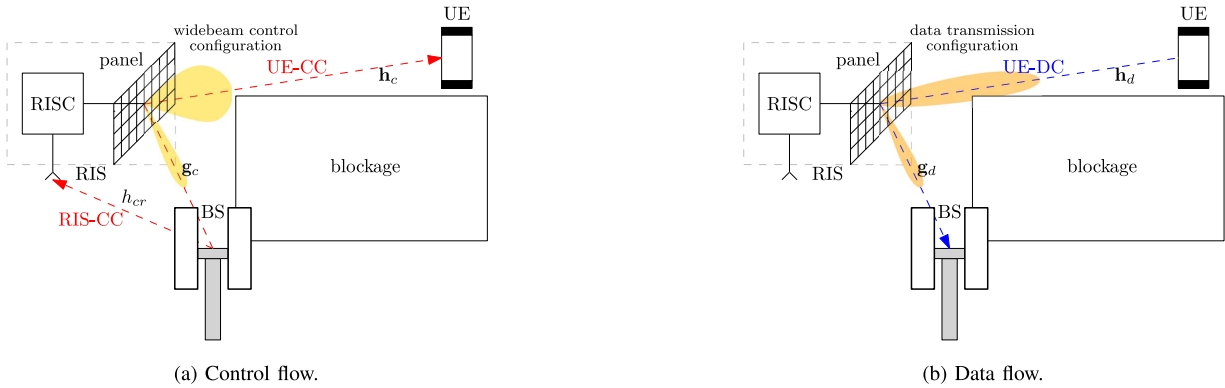


**FIGURE 1.** Setup of interest: an RIS extends the coverage of the BS which has a blocked link to the UE. During control signaling, the RIS loads a control (ctrl) configuration to the RIS to deliver low-rate control packets to the UE. During data transmission, the BS controls and communicates with the RIS to load a certain configuration to achieve a desired communication performance.

the coherence time of the DC. If the scenario exhibits high channel coherence time, the OPT-CE paradigm delivers superior data rate performance. However, its feasibility diminishes when the channel experiences rapid changes due to the increased control overhead. In contrast, the CB-BSW paradigm generally provides a lower data rate but proves suitable for scenarios with low coherence time due to its reduced control overhead. Additionally, our findings indicate that the reliability of control signaling is minimally affected by the paradigm used when the RIS-CC is an OB-CC. However, when an IB-CC serves as RIS-CC, the results reveal that OPT-CE control is less reliable than CB-BSW due to the increased complexity associated with the former.

*Paper outline:* Section II presents the system model. Section III describes the transmission paradigms and their performance assuming error-free CCs. Section IV shows how to analyze the impact of CCs design in the communication performance, whose results are shown in Section V. Section VI discusses how to relax some of the simplification assumptions made in this paper, while Section VII concludes the paper.

*Notation:* Lower and upper case boldface letters denote vectors and matrices, respectively. Calligraphic letters denote sets, whose cardinality is  $|\cdot|$ . The Euclidean norm of  $\mathbf{x}$  is  $\|\mathbf{x}\|$ ;  $\odot$  denotes the element-wise product.  $\mathcal{P}(\cdot)$  is the probability of an event,  $\mathbb{E}[\cdot]$  is the expected value;  $\mathcal{CN}(\boldsymbol{\mu}, \mathbf{R})$  is the complex Gaussian distribution with mean  $\boldsymbol{\mu}$  and covariance matrix  $\mathbf{R}$ ,  $\text{Exp}(\lambda)$  is the exponential distribution with mean value  $1/\lambda$ .  $\lfloor a \rfloor$  is the nearest lower integer of  $a$ ;  $\mathbb{N}$  and  $\mathbb{C}$  are the set of natural and complex numbers;  $\Re\{\cdot\}$  returns the real part of a complex number, and  $j \triangleq \sqrt{-1}$ .

## II. SYSTEM MODEL

This section introduces a simplified communication model involving an RIS. We focus on the uplink (UL) scenario depicted in Fig. 1, which comprises a single-antenna BS, a single-antenna UE, and a solely reflective RIS [8]. The primary aim of this system is to facilitate efficient data communication between the UE and the BS with the support

of the RIS. To accomplish this, the BS establishes control signaling links with both the RIS and the UE. The details and the key assumptions are given below.

### A. RIS OPERATION MODEL

The internal operations of the RIS are divided into the RIS panel and the RISC. The panel comprises  $N$  elements equally spaced on a planar surface. The surface is solely reflective, implying that each element only controls the reflection properties of the incoming waves and that the RIS cannot process any of them. In particular, we focus on configuring the phases of the elements to change the reflection angle of an incoming wave, where their phase shifts are denoted as  $\varphi_n \in [0, 2\pi]$ ,  $\forall n \in \mathcal{N} = \{1, \dots, N\}$ .<sup>1</sup> We denote as  $\boldsymbol{\phi} = [e^{j\varphi_1}, \dots, e^{j\varphi_N}]^T \in \mathbb{C}^N$  the vector representing a particular configuration, i.e., the set of phase shifts configured at the metasurface's elements at a given time. The RISC is in charge of loading different configurations to the RIS surface. Without loss of generality, we indicate as  $\tau_s \in \mathbb{R}_+$  the time needed to switch to a new configuration. Moreover, the RISC is equipped with a communication module, which is used to exchange control signals with the BS. We refer to the link connecting the RISC to the BS as the RIS-CC. We consider that the RISC stores a look-up table containing a set of predefined configurations, namely the *common codebook* of configurations,  $\mathcal{C} = \{\boldsymbol{\phi}_1, \dots, \boldsymbol{\phi}_C\}$ ,  $|\mathcal{C}| = C$ , that can be designed according to the task at hand; a copy of  $\mathcal{C}$  is stored in the BS as well. The control signals between the BS and the RISC can then be based on indexing elements of  $\mathcal{C}$  or by explicitly sending a configuration  $\boldsymbol{\phi}$ , if the BS wants to load a configuration not present in the common codebook, i.e.,  $\boldsymbol{\phi} \notin \mathcal{C}$ . In the next sections,  $\mathcal{C}$  is going to be defined more explicitly according to OPT-CE and CB-BSW paradigms.

<sup>1</sup>For the sake of simplicity and following the standard practice in literature, we consider an ideal RIS to show the theoretical performance achievable by the system at hand. We expect that more realistic models addressing attenuation, mutual coupling, quantization, and non-linear effects would reduce the overall performance [8].

## B. UE COMMUNICATION MODEL

To analyze the communication performance, we assume a frame-based fixed time system of  $\tau \in \mathbb{R}_+$  seconds. The frame is further divided into phases that organize the signals exchanged at a given time. Within a frame, control and data information are exchanged in different phases. In each frame, the UE communicate with the BS through the RIS: it transmits payload data using the UE-DC, while the exchange of control messages uses the UE-CC. To ensure mathematical tractability, ideal timing and frequency synchronization among devices at the PHY layer is assumed. Perfect synchronization is also considered at the frame level across these devices. Also, we consider that the RIS can be configured at any time within a frame, and we make the following assumption about the behavior of the RIS when the BS and the UE exchange control information.

Assumption 1 (RIS ctrl configuration): To allow control signaling exchange between the BS and the UE, we consider that the RIS loads a *control (ctrl) configuration* that ensures that control messages traveling through the UE-CC reach the destination.<sup>2</sup> Without loss of generality, we assume that the RISC loads the ctrl configuration when in idle, *i.e.*, anytime it does not receive any explicit command from the BS.

## C. CHANNEL MODELS

We adopt the block fading model at a frame level, implying that the channel conditions remain constant throughout the frame duration. Remark that this binds the frame duration  $\tau$  to the channel coherence time: the higher the coherence time, the longer the frame duration. The following assumption is made on the channels, further described in the sequel.

Assumption 2 (Narrowband channels): To allow a simple analysis of both control and data channels, the three channels under consideration – 1) the UE-DC, 2) the UE-CC, and 3) the RIS-CC – are considered to be narrowband.<sup>3</sup>

### 1) UE-DC

This channel operates at a central frequency  $f_d$  with a bandwidth of  $B_d$ . The UL SNR can be calculated as:

$$\gamma = \frac{\rho_u}{\sigma_b^2} \left| \boldsymbol{\phi}^T (\mathbf{h}_d \odot \mathbf{g}_d) \right|^2 = \frac{\rho_u}{\sigma_b^2} \left| \boldsymbol{\phi}^T \mathbf{z}_d \right|^2, \quad (1)$$

where  $\mathbf{h}_d \in \mathbb{C}^N$  and  $\mathbf{g}_d \in \mathbb{C}^N$  are the gains of UE-RIS and RIS-BS links, respectively. We further define the equivalent DC as  $\mathbf{z}_d = \mathbf{h}_d \odot \mathbf{g}_d \in \mathbb{C}^N$ . The UE transmit power is  $\rho_u$ , and  $\sigma_b^2$  is the noise power at the BS radio frequency (RF) chain.<sup>4</sup>

<sup>2</sup>The design of the ctrl configuration is out of the scope of this paper; potential candidates for ctrl configurations are wide-width beams and hierarchical radiation patterns, which generally offer good reliability and coverage when low data rates are needed [23], [46], [47].

<sup>3</sup>The analysis can be straightforwardly extended to a wideband transmission, as discussed in Section VI.

<sup>4</sup>In the remainder of the paper, we assume that the BS knows the transmit and noise powers in this section, *i.e.*,  $\rho_u$ ,  $\rho_b$ ,  $\sigma_r^2$ ,  $\sigma_u^2$  and  $\sigma_b^2$ ; the transmit powers are usually determined by the protocol or by the BS itself; the noise powers can be considered static for a long time horizon and hence estimated previously through standard estimation techniques, *e.g.*, [48].

The configurations  $\boldsymbol{\phi}$  supporting the UE-DC are subject to design and will be further specified in the following sections.

### 2) UE-CC

This channel operates at central frequency  $f_u$  with a bandwidth of  $B_u$ . The UE-CC channel is defined as

$$h_{cu} = \boldsymbol{\phi}_{\text{ctrl}}^T (\mathbf{h}_c \odot \mathbf{g}_c) = \boldsymbol{\phi}_{\text{ctrl}}^T \mathbf{z}_c, \quad (2)$$

where  $\boldsymbol{\phi}_{\text{ctrl}}$  is the ctrl configuration (see Assumption 1) and  $\mathbf{h}_c \in \mathbb{C}^N$  and  $\mathbf{g}_c \in \mathbb{C}^N$  are the gains of the UE-RIS and RIS-BS links, respectively. The equivalent end-to-end channel is  $\mathbf{z}_c = \mathbf{h}_c \odot \mathbf{g}_c \in \mathbb{C}^N$ . We consider a worst-case scenario where the channel (2) has no line-of-sight (LoS) component, *i.e.*, it is distributed as  $h_{cu} \sim \mathcal{CN}(0, \tilde{\lambda}_u)$ ;  $\tilde{\lambda}_u$  is a term accounting for the large-scale fading – known by the BS – which is dependent on the ctrl configuration design. Hence, the instantaneous SNR measured at the UE is

$$\Gamma_u = \frac{\rho_b}{\sigma_u^2} |h_{cu}|^2 \sim \text{Exp}\left(\frac{1}{\tilde{\lambda}_u}\right), \quad (3)$$

where  $\lambda_u = \frac{\rho_b \tilde{\lambda}_u}{\sigma_u^2}$  denotes the average SNR at the UE, being  $\rho_b$  the BS transmit power and  $\sigma_u^2$  the UE's RF chain noise power. We make the following assumption on this channel.

Assumption 3: [UE-CC design]

We assume that the UE-CC operates as an IB-CC, meaning that the frequency  $f_u$  matches the frequency  $f_d$ , and the physical resources allocated for the UE-CC coincide with those utilized for the UE-DC. This assumption is based on the premise that any UE-CC signal must travel through the RIS and the RIS operates at the same data frequency and bandwidth.

### 3) RIS-CC

This narrowband channel operates on central frequency  $f_r$  with bandwidth  $B_r$ . Let  $h_{cr} \in \mathbb{C}$  denote the channel coefficient of the RIS-CC. To obtain simple analytical results, we assume that  $h_{cr} \sim \mathcal{CN}(0, \tilde{\lambda}_r)$ , where  $\tilde{\lambda}_r$  accounts for the large-scale fading, assumed known by the BS. Hence, the instantaneous SNR measured at the RISC is

$$\Gamma_r = \frac{\rho_b}{\sigma_r^2} |h_{cr}|^2 \sim \text{Exp}\left(\frac{1}{\tilde{\lambda}_r}\right), \quad (4)$$

where  $\lambda_r = \frac{\rho_b \tilde{\lambda}_r}{\sigma_r^2}$  denotes the average SNR with  $\sigma_r^2$  being the noise power at the RISC RF chain. We make the following assumption on the RIS-CC.

Assumption 4 (RIS-CC design): The RIS-CC can either be: *i*) IB-CC, implying that the physical resources employed by this channel are overlapping with the one used by the UE-DC, *i.e.*,  $f_r = f_d$ ; or *ii*) OB-CC, where the physical resources are orthogonal, *e.g.*, simulating a wired connection between the BS and the RISC. In the case of OB-CC, we further assume that the RIS-CC is an error-free channel, *i.e.*,  $\lambda_r \rightarrow \infty$ , with feedback capabilities since the system designer can easily make the RIS-CC as reliable as possible.

### III. RIS-ENABLED COMMUNICATION PARADIGMS

In this section, we first describe the structure and building blocks of a generic RIS-enabled communication paradigm. We use this to instantiate two particular co strategies belonging to the OPT-CE and the CB-BSW paradigms, representing the multiplexing and diversity paradigms introduced in Section I-B. We analyze their performance in terms of the expected SNR and spectral efficiency (SE), while specifying the errors eventually occurring during their operations.

#### A. GENERIC STRUCTURE

In a system without RISs, a generic structure for a typical communication strategy can be divided into three key phases occurring in every frame: “*Signaling*,” “*Algorithmic*,” and “*Payload*.” The Signaling phase encompasses the actions conducted on the CCs required for network node control. This phase relies on the quality of the CCs and the information content within the control messages. The Algorithmic phase involves processing operations aiming at optimizing transmission parameters, such as selecting the transmit SE. The specifics of this phase are contingent on the chosen communication paradigm. The Payload phase handles the actual data transmission.

In an RIS-aided system, we identify that a generic structure would have two Signaling phases, namely “*Initialization*” and “*Setup*,” in conjunction with the “*Algorithmic*” and “*Payload*” phases. Sequentially, we have: Initialization, Algorithmic, Setup and Payload.<sup>5</sup> The time of a frame is thus divided as  $\tau = \tau_{\text{ini}} + \tau_{\text{alg}} + \tau_{\text{set}} + \tau_{\text{pay}}$ , where  $\tau_i < \tau$ ,  $\forall i \in \{\text{ini, alg, set, pay}\}$ , is the time of the corresponding phase. The duration of each phase can vary depending on the paradigm and the kind of CCs.

##### 1) INITIALIZATION

The BS notifies the RIS and UE about the beginning of a frame over the CCs. It is assumed that the RISC loads the ctrl configuration at the start of this phase. Although not considered here, the Initialization phase can also incorporate a random access procedure (see, e.g., [28]) as an intermediate step where newly connected UEs are scheduled.

##### 2) ALGORITHMIC

This phase encompasses all the processes and computations needed to optimize the subsequent Payload phase, where the actual data transmission takes place. Objectives of this phase encompass the selection/optimization of the appropriate RIS configuration(s), while others, such as determining the transmission parameters for the UE and/or the BS, could be included. To tackle these objectives, some form of wireless environment sensing from the end nodes is required, typically enabled by the transmission of pilot sequences,

<sup>5</sup>We note that there could be communication strategies in which some of these phases may not be present, e.g., access procedures; however, the mentioned four phases set a basis for a sufficiently general procedure that can be used to investigate the design of other RIS-aided schemes, where some of the phases are merged or omitted, as discussed in Section VI.

whose specifications – their number, waveform, UL or DL transmission, etc – are defined by the communication strategy. The BS can then use the collected pilot signals and invoke pre-defined algorithms to fulfil the objectives. The outcome of these algorithms might be affected by different types of *algorithmic errors* that may prevent the system from performing as expected, and thus, should be considered when analyzing the overall performance.

##### 3) SETUP

During this phase, the RIS configuration chosen during the Algorithmic phase needs to be communicated to the RISC, which in turn commands the RIS to load it. Additionally, further control signaling may occur between the BS and the UE as a final check before data transmission to, e.g., set the modulation and coding scheme (MCS).

##### 4) PAYLOAD

Here, the actual data transmission takes place while the RIS loads the configuration specified before. This phase may or may not include feedback of the data sent by the UE at the end; this aspect is not considered in this paper. The communication performance of the considered RIS-enabled communication system is measured during this phase.

In the following subsections, we describe the operations of two communication strategies illustrating the OPT-CE and CB-BSW paradigms, respectively, using the generic structure defined above. Then, we investigate their Algorithmic phases, analyzing their performance and possible errors. The first strategy (OPT-CE) follows a multiplexing transmission: the UE’s CSI is evaluated at the BS and then exploited to compute the RIS’ optimal configuration and the corresponding achievable data rate. Then, the transmission is made using the optimized configuration and MCS. The second approach (CB-BSW) resembles the concept of diversity transmission: the BS selects a target KPI *a priori*; then, it instructs the RISC to sweep through a set of predefined configurations while the UE transmits replicas of a pilot sequence; then, the data transmission is made using a configuration satisfying the target KPI, if exists, or an outage occurs. Fig. 2 shows the data exchange diagrams of the two paradigms.

### B. OPTIMIZATION BASED ON CHANNEL ESTIMATION (OPT-CE)

In OPT-CE, the BS needs to obtain the CSI for the UE to optimize the RIS configuration. The necessary measurements can be collected by transmitting pilot sequences from the UE. During the Initialization phase, the BS informs the other entities that the procedure is starting. First, the UE is informed through the UE-CC to prepare to send pilots. Second, to solve the indeterminacy of the  $N$ -path CE due to the RIS presence [11], the RIS is instructed to sweep through a common codebook of configurations during the Algorithmic phase, called *CE codebook* and denoted as  $\mathcal{C}_{\text{CE}} \subseteq \mathcal{C}$ . To change between the configurations in the CE codebook, we consider that the BS needs to send only a single control

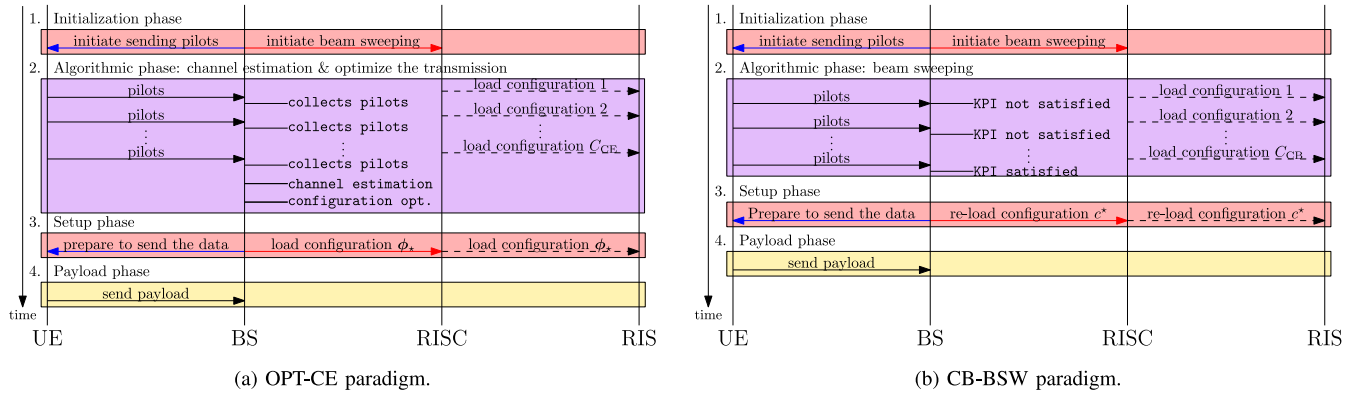


**FIGURE 2.** Data exchange diagram of the two RIS-enabled communication paradigms. Signals traveling through RIS-CC, UE-CC, and UE-DC are represented by solid red, solid blue, and solid black lines, respectively. RISC to RIS commands are indicated with dashed black lines. BS operations are in `monospace font`.

message to the RISC since the RIS sweeps following the order stipulated by the codebook. During the Algorithmic phase, the UE sends replicas of its pilot sequence, subject to different RIS configurations, to let each of them experience a different propagation environment. After a sufficient number of samples is received, the BS estimates the CSI and compute the optimal RIS's configuration [7], [8]. Then, the Setup phase starts, in which the BS exploit the ctrl configuration<sup>6</sup> to transmit over the UE-CC and instructing the UE to start sending data. Subsequently, the BS informs the RISC, over the RIS-CC, to load the optimal configuration. Finally, the Payload phase takes place.

### 1) ANALYTICAL PERFORMANCE ANALYSIS

We now present the CE procedure and analyze its performance in connection to the cardinality of the employed codebook  $C_{CE} = |C_{CE}|$ . As an example, we employ [11] in a single-user setting to describe a general CE procedure.<sup>7</sup> Let us start with the pilot sequence transmission and its processing. We denote a single pilot sequence as  $\psi \in \mathbb{C}^p$ , spanning  $p$  symbols and having  $\|\psi\|^2 = p$ . Every time a configuration from the codebook is loaded at the RIS, the UE sends a replica of the sequence  $\psi$  towards the BS. When the configuration  $c \in C_{CE}$  is loaded, the following signal is received at the BS

$$\mathbf{y}_c^T = \sqrt{\rho_u} \phi_c^T \mathbf{z}_d \psi^T + \tilde{\mathbf{w}}_c^T \in \mathbb{C}^{1 \times p}, \quad (5)$$

where  $\phi_c$  denotes the phase profile vector of the configuration  $c \in C_{CE}$ ,  $\rho_u$  is the transmit power, and  $\tilde{\mathbf{w}}_c \sim$

<sup>6</sup>We remark that the ctrl configuration is automatically loaded after the Algorithmic phase ends due to the idle state of the RIS. Another approach is loading the optimal configuration evaluated in the Algorithmic phase also to send the control information toward the UE; nevertheless, the RISC needs to be informed previously by a specific control message by the BS. We do not consider this approach to keep the frame structure of the two paradigms similar, thereby simplifying the analysis and the presentation in Section IV.

<sup>7</sup>This procedure is representative of more sophisticated CE methods that may further exploit channel rank deficiency, parametric estimation of structured channel models, or compressive sensing of sparse channel representation for the estimation algorithm employed at the BS [12]. Regardless of the exact method and processing employed, the overall procedure follows the steps described in the remainder of the section.

$\mathcal{CN}(0, \sigma_b^2 \mathbf{I}_p)$  is the additive white gaussian noise (AWGN). The received symbol is then correlated with the pilot sequence and normalized by  $\sqrt{\rho_u p}$ , yielding

$$y_c = \frac{1}{\sqrt{\rho_u p}} \mathbf{y}_c^T \psi^* = \phi_c^T \mathbf{z}_d + w_c \in \mathbb{C}, \quad (6)$$

where  $w_c \sim \mathcal{CN}(0, \frac{\sigma_b^2}{\rho_u p})$  is the resulting AWGN.<sup>8</sup> The pilot transmissions and the processing in (6) are repeated for all RIS configurations, *i.e.*,  $\forall c \in C_{CE}$ . The resulting signal  $\mathbf{y} = [y_1, y_2, \dots, y_{C_{CE}}]^T \in \mathbb{C}^{C_{CE}}$  can be then compactly written in the following form:

$$\mathbf{y} = \Theta^T \mathbf{z}_d + \mathbf{w}, \quad (7)$$

where  $\Theta = [\phi_1, \phi_2, \dots, \phi_{C_{CE}}] \in \mathbb{C}^{N \times C_{CE}}$  is the matrix containing all the configurations used and  $\mathbf{w} = [w_1, \dots, w_{C_{CE}}]^T \in \mathbb{C}^{C_{CE}}$  is the AWGN term. For the sake of generality, we will assume that there is no prior information about the channel distribution at the BS. Therefore, we cannot estimate separately  $\mathbf{h}_d$  and  $\mathbf{g}_d$ , but only the cascade channel  $\mathbf{z}_d$ . It is possible to show that a necessary (but not sufficient) condition to perfectly estimate the channel coefficients for an unstructured channel model is that  $C_{CE} \geq N$  to have a linearly independent set of equations, obtained by constructing the configuration codebook for CE to be at least of rank  $N$  [11], [12]. As a possible solution, we can use the discrete Fourier transform (DFT) matrix, *i.e.*,  $[\Theta]_{n,c} = e^{-j2\pi \frac{(n-1)(c-1)}{C_{CE}}}$ , with  $n \in \mathcal{N}$ ,  $c \in C_{CE}$ , and  $\Theta^* \Theta^T = C_{CE} \mathbf{I}_N$ . Considering that the parameter vector of interest is deterministic, the least-squares estimate yields the estimation [50]

$$\hat{\mathbf{z}}_d = \frac{1}{C_{CE}} \Theta^* \mathbf{y} = \mathbf{z}_d + \mathbf{n}, \quad (8)$$

<sup>8</sup>The consideration of dividing the pilot transmission over configurations over small blocks of  $p$  symbols serves three purposes: *i)* from the hardware point of view, it might be difficult to change the phase-shift profile of an RIS within the symbol time, *ii)* to reduce the impact of the noise, and *iii)* to have the possibility of separating up to  $p$  UE's data streams, if the pilots are designed to be orthogonal to each other [49].

where  $\mathbf{n} \sim \mathcal{CN}(0, \frac{\sigma_b^2}{\rho_u C_{CE}} \mathbf{I}_N)$ , and whose performance is proportional to  $1/C_{CE}$ .

Based on the acquired CSI, the BS can evaluate the configuration  $\phi_*$  that maximizes the instantaneous SNR of the UE, by solving

$$\phi_* = \max_{\phi} \left\{ \left| \phi^T \hat{\mathbf{z}}_d \right|^2 \mid \|\phi\|^2 = N \right\}. \quad (9)$$

Although problem (9) is not convex, it can be solved through the use of Cauchy-Schwarz inequality, as shown in [7], [17], which turns out to provide the intuitive setting  $(\phi_*)_n = e^{-j\angle(\hat{\mathbf{z}}_d)_n}$ ,  $\forall n \in \mathcal{N}$ . In words, each RIS element should phase shift its reflected signal so that it sums coherently in phase with the signals reflected from the other RIS elements at the BS [7]. The resulting UL estimated SNR at the BS is:

$$\hat{\gamma}_{CE} = \frac{\rho_u}{\sigma_b^2} \left| \phi_*^T \hat{\mathbf{z}}_d \right|^2. \quad (10)$$

Based on the estimated SNR, the SE of the data communication can be adapted to be the maximum achievable, *i.e.*,

$$\eta_{CE} = \log_2(1 + \hat{\gamma}_{CE}). \quad (11)$$

## 2) ALGORITHMIC ERRORS

For the OPT-CE paradigm, a communication outage occurs in the case of an *overestimation error*, *i.e.*, if the selected SE  $\eta_{CE}$  is higher than the actual channel capacity, leading to an unachievable communication rate [51]. The probability of this event is

$$p_{ae} = \mathcal{P}[\eta_{CE} = \log(1 + \hat{\gamma}_{CE}) \geq \log_2(1 + \gamma_{CE})], \quad (12)$$

where  $\gamma_{CE} = \frac{\rho_u}{\sigma_b^2} |\phi_*^T \mathbf{z}_d|^2$  is the actual SNR at the BS. Eq. (12) translates to the condition

$$p_{ae} = \mathcal{P}[\hat{\gamma}_{CE} \geq \gamma_{CE}] = \mathcal{P}\left[ \left| \phi_*^T \mathbf{z}_d + \phi_*^T \mathbf{n} \right|^2 \geq \left| \phi_*^T \mathbf{z}_d \right|^2 \right]. \quad (13)$$

A detailed analysis of (13) relies on the channel model of  $\mathbf{z}_d$ , and thereby on a prior assumption about the scenario (*e.g.*, [52]); we therefore numerically evaluate the impact of the OPT-CE algorithmic error.

## C. CODEBOOK-BASED BEAM SWEEPING (CB-BSW)

In CB-BSW, the BS now does not require explicit CSI of the UE. In the Initialization phase, the BS commands the start of a new frame by signaling to the RIS and the UE. A *beam sweeping (BSW) process*, *i.e.*, an RIS configuration selection, is performed during the Algorithmic phase. This process comprises the UE sending reference signals, while the BS commands the RIS to change its configuration at regular periods accordingly to a set of predefined configurations, labeled as the *BSW codebook* denoted by  $\mathcal{C}_{CB} \subseteq \mathcal{C}$ . The BS receives the reference signals that are used to measure UE's KPI. The BSW process is triggered when a single BS control message is received by the RISC. At its end, the BS selects a configuration satisfying the target KPI. During the Setup

phase, the BS informs the UE over the UE-CC to prepare to send data, while the RIS uses the ctrl configuration, and informs the RISC through the RIS-CC to load the selected configuration. Finally, the Payload phase takes place.

Remark 1 (Fixed vs Flexible frames): The BSW process during the Algorithmic phase may make use of i) a *fixed* or ii) a *flexible* frame structure. The fixed frame ends after a fixed number of BSW codebook configurations have been loaded. The flexible frame structure allows stopping the BSW as soon as a KPI value measured is above the target one. Flexible frame requires on-the-fly KPI measurements at the BS, while UE-CC needs to be reserved to promptly inform the UE about the frame termination when the target KPI is met, thus modifying the overall frame (see Section IV).

## 1) ANALYTICAL PERFORMANCE ANALYSIS

For CB-BSW, we assume that the target KPI is a target SNR  $\gamma_0$  measured at the BS via the average received signal strength (RSS) metric. In this case, a fixed SE is considered *a priori*, which is given by

$$\eta_{CB} = \log_2(1 + \gamma_0), \quad (14)$$

and the goal is find a configuration from the RIS codebook that supports it. We analyze the system performance starting from the pilot sequence transmission and processing. As before, every pilot sequence consists of  $p$  symbols.<sup>9</sup> Once again, we denote a single sequence as  $\psi \in \mathbb{C}^p$  having  $\|\psi\|^2 = p$ . After the RIS loads configuration  $c \in \mathcal{C}_{CB}$ , the UE sends a replica of  $\psi$  and, similar to (5), the BS receives the signal:

$$\mathbf{y}_c^T = \sqrt{\rho_u} \phi_c^T \mathbf{z}_d \psi^T + \tilde{\mathbf{w}}_c^T \in \mathbb{C}^{1 \times p}, \quad (15)$$

where  $\phi_c$  denotes the configuration  $c \in \mathcal{C}_{CB}$ . The received signal is then correlated with  $\psi$  and normalized by  $p$ :

$$y_c = \frac{1}{p} \mathbf{y}_c^T \psi^* = \sqrt{\rho_u} \phi_c^T \mathbf{z}_d + w_c \in \mathbb{C}, \quad (16)$$

where  $w_c \sim \mathcal{CN}(0, \frac{\sigma_b^2}{p})$  is the resulting AWGN. The SNR provided by the configuration can be estimated as follows:

$$\hat{\gamma}_c = \frac{|y_c|^2}{\sigma_b^2} = \underbrace{\frac{\rho_u}{\sigma_b^2} |\phi_c^T \mathbf{z}_d|^2}_{\gamma_c} + 2\Re \left\{ \frac{\sqrt{\rho_u}}{\sigma_b^2} \phi_c^T \mathbf{z}_d w_c \right\} + \frac{|w_c|^2}{\sigma_b^2}, \quad (17)$$

where  $|w_c|^2 \sigma_b^{-2} \sim \text{Exp}(p)$ . It is worth noting that the estimated SNR is affected by the exponential error generated by the noise, but also by the error of the mixed product between the signal and the noise, whose probability distribution function (pdf) depends on the pdf of  $\mathbf{z}_d$ . Based on (17), we can select the best configuration  $c^* \in \mathcal{C}_{CB}$  providing the

<sup>9</sup>The pilot sequences for OPT-CE and CB-BSW can be different and have different lengths. In practice, they should be designed and optimized for each of those approaches, which is beyond the scope of this paper. We use the same pilot sequence length notation in both paradigms for simplicity.



target KPI. According to Remark 1, we next discuss the selection of the configuration for the two different frame structures.

**Fixed Frame.** When the frame has a fixed structure, the BSW procedure ends after the RIS sweeps through the whole codebook. In this case, we can measure the KPIs for all available configurations. The configuration selected for the payload phase is the one achieving the highest estimated SNR among the ones satisfying the target KPI  $\gamma_0$ , as

$$c^* = \arg \max_{c \in C_{CB}} \{\hat{\gamma}_c \mid \hat{\gamma}_c \geq \gamma_0\}. \quad (18)$$

If no configuration achieves the target KPI, the communication is not feasible, and we run into an outage event.

**Flexible Frame.** When the frame has a flexible structure, the end of the BSW process is triggered by the BS when the measured KPI reaches the target value. A simple on-the-fly selection method involves testing if the estimated SNR is greater than the target  $\gamma_0$ ; *i.e.*, after eq. (17) is obtained for configuration  $c \in C_{CB}$ , we set

$$c^* = c \iff \hat{\gamma}_c \geq \gamma_0. \quad (19)$$

As soon as  $c^*$  is found, the BS communicates to both RIS and UE that the Payload phase can start; otherwise, the BSW process continues until a configuration is selected. If no configuration of the codebook  $C_{CB}$  satisfies the condition (19), then communication is not feasible and an outage occurs.

## 2) ALGORITHMIC ERRORS

For the CB-BSW paradigm, an outage event occurs when no configuration in the BSW codebook satisfies the target KPI, and when the selected configuration provides an SNR lower than the target one, although the estimated SNR was higher; we denote the latter as the overestimation event. These two events are mutually exclusive, and hence, their probability is

$$\begin{aligned} p_{ae} &= \mathcal{P}[\gamma_{c^*} \leq \gamma_0 \mid \hat{\gamma}_{c^*} > \gamma_0] + \mathcal{P}[\hat{\gamma}_c \leq \gamma_0, \forall c \in C_{CB}] \\ &= \mathcal{P}\left[\hat{\gamma}_{c^*} - \gamma_0 \leq \frac{|w_{c^*}|^2}{\sigma_b^2} + 2\Re\left\{\frac{\sqrt{\rho_u}}{\sigma_b^2} \phi_{c^*}^\top \mathbf{z}_d w_c\right\}\right] \\ &\quad + \mathcal{P}[\hat{\gamma}_1 \leq \gamma_0, \dots, \hat{\gamma}_{C_{CB}} \leq \gamma_0], \end{aligned} \quad (20)$$

where  $\gamma_{c^*} = \frac{\rho_u}{\sigma_b^2} |\phi_{c^*}^\top \mathbf{z}_d|^2$  is the actual SNR and  $\hat{\gamma}_{c^*} - \gamma_0 > 0$ . By applying Chebychev inequality, the overestimation probability (first term) can be upper bounded by

$$\mathcal{P}\left[\hat{\gamma}_{c^*} - \gamma_0 \leq \frac{|w_{c^*}|^2}{\sigma_b^2} + 2\Re\left\{\frac{\sqrt{\rho_u}}{\sigma_b^2} \phi_{c^*}^\top \mathbf{z}_d w_c\right\}\right] \leq \frac{p^{-1}}{\hat{\gamma}_{c^*} - \gamma_0}, \quad (21)$$

from which we infer that the higher the gap between  $\hat{\gamma}_{c^*}$  and  $\gamma_0$ , the lower the probability of error. The CB-BSW employing the fixed structure generally has a higher value of  $\hat{\gamma}_{c^*} - \gamma_0$  than the one with the flexible structure due to the use of the arg max operator to select the configuration

$c^*$ . Therefore, the fixed structure is generally more robust to overestimation errors. On the other hand, the evaluation of the probability that no configuration in the beam sweeping codebook satisfies the target KPI requires the knowledge of the cumulative density function (CDF) of the estimated SNR, whose analytical expression is channel-model dependent and generally hard to obtain. Here, we also resort to numerical evaluation of the impact of the CB-BSW algorithmic errors.

## D. TRADE-OFFS IN DIFFERENT TRANSMISSION PARADIGMS

The two aforementioned RIS-aided transmission paradigms can be seen as a generalization of the *adaptive rate* (multiplexing) and *fixed rate* (diversity) transmission approaches. Essentially, the SE of the OPT-CE is adapted to the achievable rate under the optimal configuration (see (11)), while the SE of the CB-BSW is set *a priori* according to the target KPI (see (14)). Comparing (11) and (14) under the same environmental conditions, we have that

$$\eta_{CB} \leq \eta_{CE}, \quad (22)$$

where the price to pay for the higher SE of the OPT-CE paradigm is the increased overhead. OPT-CE needs an accurate CSI for reliable rate adaptation, which translates into a higher number of pilot sequences to be transmitted by the UE compared to CB-BSW. Furthermore, additional time and processing are required to determine the optimal configuration of the RIS. Consequently, the SE of data transmission alone cannot be considered a fair comparison metric, as it does not consider the overheads generated by the communication paradigms.

## IV. IMPACT OF THE CONTROL CHANNELS

In this section, we define a performance metric that simultaneously measures the communication performance and the impact of control signaling. Then, we characterize the terms of this metric concerning overhead and reliability of the control signaling for the presented paradigms, and for the different CCs.

### A. UTILITY FUNCTION DEFINITION

To measure the communication performance, we define a utility function that takes into account a) the overhead and the error of the communication paradigms and b) the reliability of the CCs. Regarding the former, we define the *goodput*  $R$  as a discrete random variable whose value depends on the communication paradigm and its algorithmic errors:

$$R(\tau_{\text{pay}}, \eta) = \begin{cases} \frac{\tau_{\text{pay}}}{\tau} B_d \eta, & \text{with prob. } 1 - p_{ae}, \\ 0, & \text{with prob. } p_{ae}, \end{cases} \quad (23)$$

In this expression,  $\eta = \eta_{CE}$  in (11) or  $\eta = \eta_{CB}$  in (14) if OPT-CE or CB-BSW is respectively employed,  $\tau_{\text{pay}}$  is the duration of the payload phase, and  $\tau$  is the overall frame duration. The overall overhead time is the sum of the time to carry out the Initialization, Algorithmic, and Setup phases,

denoted as  $\tau_{\text{ini}}$ ,  $\tau_{\text{alg}}$ , and  $\tau_{\text{set}}$ , respectively.<sup>10</sup> Accordingly, the payload time can be written as

$$\tau_{\text{pay}} = \tau - \tau_{\text{ini}} - \tau_{\text{alg}} - \tau_{\text{set}}. \quad (24)$$

While the overall frame length is fixed, the choice of transmission paradigm impacts the overhead time, which is a function of: the number of transmitted pilots and their duration  $\tau_p$ ; the optimization time  $\tau_A$ ; the time required for the transmission of the control packets to the UE and RISC,  $\tau_i^{(u)}$  and  $\tau_i^{(r)}$ , respectively; the time needed by the RIS to switch configurations  $\tau_s$ .

Regarding the reliability of the CCs, we denote as  $P = P_u + P_r$  the total number of control packets needed to let a communication paradigm work, where  $P_u$  and  $P_r$  are the numbers of control packets intended for the UE and the RISC, respectively. Whenever one of such packets is erroneously decoded or lost, an event of *erroneous control* occurs. We assume that these events are independent of each other (and of the algorithmic errors). We denote the probability of erroneous control on the packet  $i$  toward entity  $k \in \{u, r\}$  as  $p_i^{(k)}$ , with  $i \in \{1, \dots, P_k\}$  and  $k \in \{u, r\}$ . Erroneous controls may influence the overhead time and the communication performance: the RIS configuration might change unpredictably,<sup>11</sup> leading to a degradation of the performance, or worse, letting the data transmission fail. While losing a single control packet may be tolerable depending on its content, we assume all control packets must be received correctly to make the communication successful. In other words, no erroneous control event is allowed. Consequently, the probability of correct control is

$$p_{\text{cc}} = \prod_{k \in \{u, r\}} \prod_{i=1}^{P_k} (1 - p_i^{(k)}). \quad (25)$$

We can include the control reliability in the communication performance, taking into account the probability of correct control in the goodput metric in (23). By assuming that the control and algorithmic errors are independent, the goodput is re-expressed as follows:

$$R(\tau_{\text{pay}}, \eta) = \begin{cases} \frac{\tau_{\text{pay}}}{\tau} B_d \eta, & \text{with prob. } p_{\text{cc}}(1 - p_{\text{ae}}), \\ 0, & \text{with prob. } 1 - p_{\text{cc}}(1 - p_{\text{ae}}), \end{cases} \quad (26)$$

Hence, the performance of the considered RIS-enabled communication system can be described by averaging  $R$  w.r.t. the control, obtaining the following *utility function*:

$$U(\tau_{\text{pay}}, \eta) = p_{\text{cc}}(1 - p_{\text{ae}}) \left( 1 - \frac{\tau_{\text{ini}} + \tau_{\text{alg}} + \tau_{\text{set}}}{\tau} \right) B_d \eta. \quad (27)$$

<sup>10</sup>We remark that the overhead time directly impacts on the latency experienced by the UE: given a fixed frame duration, a higher overhead translates into a lower time opportunity for the Payload phase, reducing the transmitted data in each slot, and hence, increasing the overall latency.

<sup>11</sup>In our scenario, if the control packet is not received, the RISC will load the ctrl configuration, *i.e.*, a predictable configuration change. However, if the RISC receives, but incorrectly decodes, a control packet, the BS cannot know which configuration, if any, will be loaded.

## B. OVERHEAD EVALUATION

Following the description of Section III, we present in Fig. 3 the frame structures of the two considered communication paradigms used to evaluate the induced overhead, where the rows represent the time horizon of the packets traveling on the different channels (first three rows) and the configuration loading time at the RISC (last row). The time horizon is obtained assuming that all the operations span multiple numbers of transmission time intervals (TTIs), each of duration of  $T$  seconds with  $\lceil \tau/T \rceil \in \mathbb{N}$  being the total number of TTIs in a frame. At the beginning of each TTI, if the RISC loads a new configuration, the first  $\tau_s$  seconds of data might be lost due to the unpredictable response of the channel during this switching period. When needed, we consider a guard period of  $\tau_s$  seconds in the overhead evaluation to avoid data disruption. Remember that the RISC loads the ctrl configuration any time it is in an idle state, *i.e.*, at the beginning of the Initialization and Setup phases.

In Fig. 3, we note that the overhead generated by the Initialization and Setup phases is *transmission paradigm independent*,<sup>12</sup> while it is *CC dependent*. Both paradigms make use of  $P = 4$  control packets,  $P_u = 2$  control packets sent on the UE-CC and  $P_r = 2$  on RIS-CC. Nevertheless, employing an OB-RIS-CC can reduce the overhead by transmitting the RIS control packets through orthogonal resources. On the other hand, the Algorithmic phase overhead is *CC independent* and *transmission paradigm dependent*, being designed to achieve the goal of the specific paradigm regardless of the CC. In the following, the overhead is evaluated.

### 1) INITIALIZATION PHASE

This phase starts with the initialization control packet sent on the UE-CC (INI-U) informing the UE that the OPT-CE procedure has started. In the IB-CC case, this is followed by the transmission of the INI-R packet to the RISC to notify the beginning of the procedure. A subsequent TTI for feedback is reserved to notify back to the BS if the INI-R packet has been received. If an OB-CC is employed, no TTI needs to be reserved because the INI-R and its feedback are scheduled simultaneously since the INI-U packet relies on different resources (see Assumption 4). The phase duration is  $\tau_{\text{ini}} = T$  or  $\tau_{\text{ini}} = 3T$  with OB- or IB-RIS-CC, respectively.

### 2) SETUP PHASE

After the optimization has run, a setup (SET-U) packet spanning one TTI is sent to the UE notifying it to prepare to send the data; then, with an IB-CC, a TTI is used to send the SET-R packet containing the information of which configuration to load during the Payload phase; a further TTI is reserved for feedback. Again, if an OB-CC is present, the SET-R and its feedback are scheduled at the same time as the SET-U packet but on different resources; therefore, no TTIs needs to be reserved for the SET-R and its feedback. Remark

<sup>12</sup>The reliability is still dependent on the paradigm (see Section IV-C).

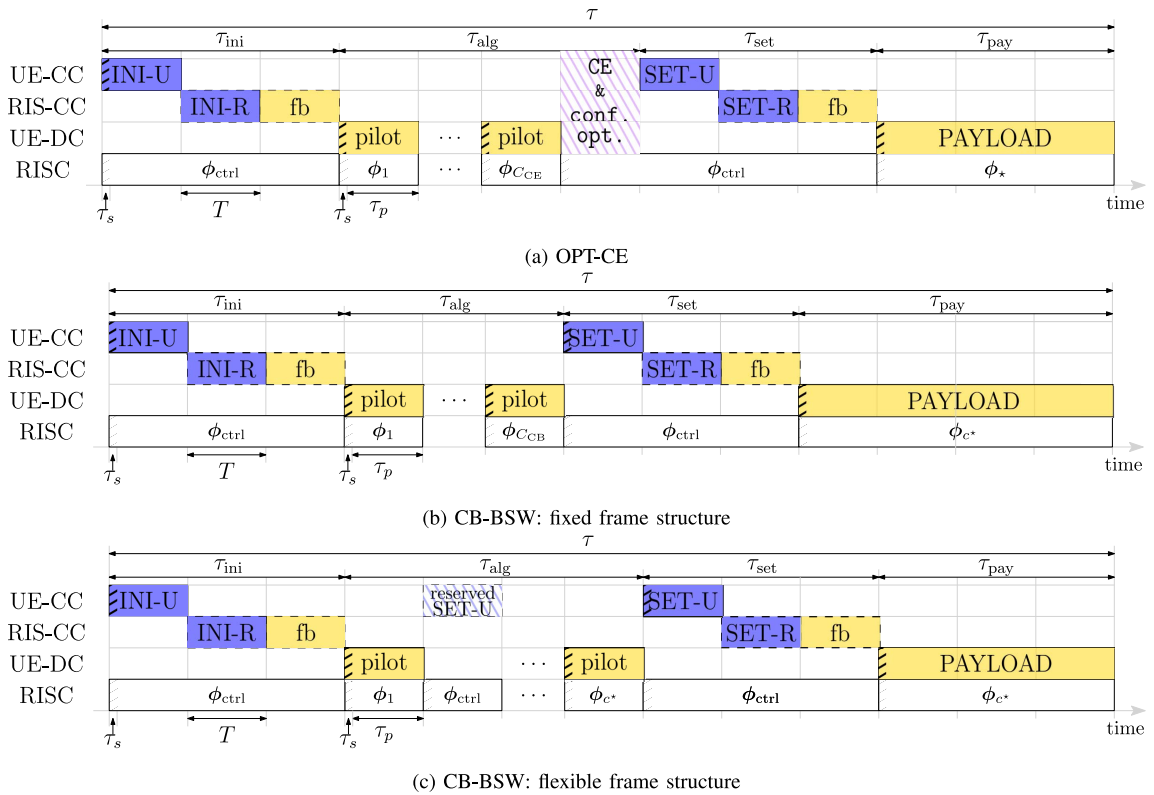


**FIGURE 3.** Frame structure for the communication paradigms under study. Packets colored in blue and in yellow have DL and UL directions, respectively; pink represents BS processing, while the white color is used to represent the RIS loaded by the RISC. Remark that INI-R (SET-R) packet and its feedback (fb) are sent at the same time of the INI-U (SET-U), but on different resources, if OB-CC is present.

that the  $\tau_s$  guard period must be considered by the UE when transmitting the data to avoid being disrupted during the load of the configuration employed in the Payload. For simplicity of evaluation, we account for this guard period in the Setup phase duration, resulting in  $\tau_{set} = \tau_{ini} + \tau_s$ .

### 3) ALGORITHMIC PHASE

This phase comprises the process of sending pilot sequences and the consequent evaluation of the configuration for the transmission. Regardless of the paradigm, we assume each pilot sequence spans an entire TTI, but the configuration's switching time must be considered a guard period. Therefore, the actual time occupied by a pilot sequence is  $\tau_p \leq T - \tau_s$  and the number of samples  $p$  of every pilot sequence is given by  $p = \lfloor \frac{T - \tau_s}{T_n} \rfloor$ , where  $T_n$  is the symbol period in seconds. Assuming that the TTI duration and the symbol period are fixed, the UE can compute the pilot length if it is informed about the guard period. The overall duration of the Algorithmic phase depends on the paradigm employed.

**OPT-CE.** In this case, the Algorithmic phase starts with  $C_{CE}$  TTIs; at the beginning of each of them, the RISC loads a different configuration, while the UE transmits replicas of the pilot sequence. After all the sequences are received, the CE process at the BS starts, followed by the configuration optimization. The time needed to perform the CE and optimization processes depends on the algorithm and the available hardware. To consider a generic case, we denote this time as  $\tau_A = AT$ .

**CB-BSW with fixed frame structure.** Similarly to the previous case, the Algorithmic phase starts with  $C_{CB}$  TTIs, at the beginning of which the RISC loads a different configuration, and the UE transmits replicas of the pilot sequence. After receiving all sequences, the BS selects the configuration as described in Section III-C. The time needed to select the configuration is considered negligible. Thus, the Setup phase may start in the TTI after the last pilot sequence is sent.

**CB-BSW with flexible frame structure.** In this case, the number of TTIs used for the beam sweeping process is not known *a priori* and depends on the measured SNR. However, to allow the system to react if the desired threshold is reached, a TTI is reserved for transmitting an acknowledgment (ACK-U) packet after each TTI used for pilot transmission. Hence, the number of TTIs needed is  $2c^* - 1$ , where  $0 < c^* \leq C_{CB}$  is a random variable.

Accordingly, the Algorithmic phase duration is

$$\tau_{alg} = \begin{cases} (C_{CE} + A) T, & \text{OPT-CE,} \\ C_{CB} T, & \text{CB-BSW fixed frame,} \\ (2c^* - 1) T, & \text{CB-BSW flexible frame.} \end{cases} \quad (28)$$

### C. RELIABILITY EVALUATION

The reliability of the control packets depends on their informative content, the time reserved for their transmission, and the bandwidth of the CC. With equal transmission time and bandwidth, transmitting a high informative packet is less

reliable than a low informative packet; similarly, increasing the time reserved leads to higher reliability. We account for this behavior via the outage probability of the  $i$ -th control packet intended to entity  $k \in \{u, r\}$ , which is given by

$$p_i^{(k)} = \Pr \left\{ \log(1 + \Gamma_k) \leq \frac{b_i^{(k)}}{\tau_i^{(k)} B_k} \right\}, \quad i = \{1, 2\}, \quad (29)$$

where  $i = 1, 2$  refers to the INI or SET packet, respectively;  $b_i^{(k)}$  is the amount of informative bits,  $\tau_i^{(k)}$  is the reserved time for transmission, and  $B_k$  is the CC bandwidth. Following the channel model in Section II, (29) can be rewritten as

$$p_i^{(k)} = 1 - \exp \left[ -\frac{1}{\lambda_k} \left( 2^{b_i^{(k)}/\tau_i^{(k)}/B_k} - 1 \right) \right]. \quad (30)$$

Plugging (30) into (25), the correct control probability is

$$p_{cc} = \exp \left[ \frac{1}{\lambda_u} \left( 2 - \sum_{i=1}^2 2^{b_i^{(u)}/\tau_i^{(u)}/B_u} \right) \right] \times \exp \left[ \frac{1}{\lambda_r} \left( 2 - \sum_{i=1}^2 2^{b_i^{(r)}/\tau_i^{(r)}/B_r} \right) \right]. \quad (31)$$

Remark that the informative content  $b_i^{(k)}$  and the reserved time  $\tau_i^{(k)}$  depend on the control packet and the communication paradigm employed due to the need to communicate different control information. Hence, different paradigms require different values of the average SNR of the UE-CC  $\lambda_u$  and the RIS-CC  $\lambda_r$  to obtain the same value of  $p_{cc}$ . In practice, the minimum  $\lambda_u$  and  $\lambda_r$  required to obtain the target correct control probability give a measure of the complexity of the decoding process. In the following, we compute  $\tau_i^{(k)}$  and  $b_i^{(k)}$  for the cases under investigation.

## 1) RESERVED TIME FOR CONTROL PACKETS

Each control packet spans an entire TTI following the data frame. However, the actual transmission time  $\tau_i^{(k)}$ , *i.e.*, the time in which informative bits can be sent without risk of being disrupted, depends on the RIS switching time. As discussed in Section IV-B, a guard period  $\tau_s$  must be considered if the RISC loads a new configuration in that TTI. Following the frame structure of Fig. 3, INI-R and SET-R packets can use the whole TTI, while INI-U packets need the guard period. The SET-U control packet does not employ the guard period under the OPT-CE, as long as  $A \geq 1$ . The guard period is needed for the CB-BSW paradigm. Hence, the transmission time of the control packets intended for the UE is  $\tau_1^{(u)} = T - \tau_s$  for all paradigms, and  $\tau_2^{(u)} = T - \tau_s$  for CB-BSW and  $\tau_2^{(u)}$  for OPT-CE, while the time reserved for the control packets intended for the RISC is  $\tau_1^{(r)} = \tau_2^{(r)} = T$ .

## 2) CONTROL PACKETS CONTENT

Without loss of generality, we can assume a common structure for all the control packets, comprising a control preamble and a control payload as depicted in Fig. 4. The preamble comprises  $b^{\text{ID}}$  bits representing the *unique*

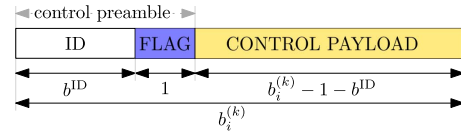


FIGURE 4. General control packet structure.

identifier (*ID*) of the destination entity in the network and a single bit flag specifying if the packet is a INI or a SET one. From the preamble, the entity can understand if the control packet is meant to be decoded and how to interpret the control payload, whose informative bits depend on the kind of control packet and on the communication paradigm considered.

**OPT-CE.** To initialize the overall procedure at the UE, the payload of the INI-U packet must contain the length of the frame  $\tau$ , the cardinality of the set  $C_{CE}$ , and the guard time  $\tau_s$ . To simplify the data transmission, the frame duration can be notified through an (unsigned) integer  $b^{\text{frame}}$  containing the number of total TTIs  $\lceil \tau/T \rceil$  set for the frame. Similarly, we can translate the guard time into an unsigned integer representing the number of guard symbols  $\lceil \tau_s/T_n \rceil$  to send  $b^{\text{guard}}$  bits. Finally, another integer of  $b^{\text{conf}}$  bits can be used to represent the cardinality  $C_{CE}$  and to notify it to the UE. Its minimum value is  $b^{\text{conf}} = \lfloor \log_2(C) \rfloor$ , where  $C$  is the total number of configurations stored in the common codebook. Similarly, the payload of the INI-R packets needs to contain the information of the length of the frame  $\tau$ , and the *set* of configuration  $C_{CE}$  to switch through. The former uses the same  $b^{\text{frame}}$  bits of the INI-U packet. To encode the latter,  $b^{\text{conf}}$  bits are used to identify a single configuration in the common codebook, and thus,  $C_{CE} b^{\text{conf}}$  needs to be transmitted to the RISC, one per desired configuration. Regarding the Setup phase, the payload of the SET-U contains only the chosen SE of the communication  $\eta_{CE}$ . This can be encoded similarly to the MCS in the 5G standard [53]: a table of predefined values indexed by  $b^{\text{SE}}$  bits. The payload of the SET-R must contain the optimal configuration  $\phi_*$ , that is, a phase-shift value for each element. Without loss of generality, we denote by  $b^{\text{quant}}$  the number of bits used to control each element, *i.e.*, the level of quantization of the RIS [4]. Hence, the overall number of informative bits is  $Nb^{\text{quant}}$ . To summarize:

$$b_i^{(k)} = b^{\text{ID}} + 1 + \begin{cases} b^{\text{frame}} + b^{\text{guard}} + b^{\text{conf}}, & k = u, i = 1, \\ b^{\text{frame}} + C_{CE} b^{\text{conf}}, & k = r, i = 1, \\ b^{\text{SE}}, & k = u, i = 2, \\ Nb^{\text{quant}}, & k = r, i = 2. \end{cases} \quad (32)$$

**CB-BSW.** The payload of the Initialization packets follows the same scheme used for the OPT-CE paradigm. The INI-U packet contains the length of the frame  $\tau$ , the cardinality of the set  $C_{CB}$ , and the guard time  $\tau_s$  in the (unsigned) integers  $b^{\text{frame}}$ ,  $b^{\text{guard}}$ , and  $b^{\text{conf}}$ , respectively. The payload of the INI-R packets contains the information of

**TABLE 1.** Simulation parameters;  $\nu$  represents the speed of light.

Scenario		
Scenario side	$D$	20 m
BS position	$\mathbf{x}_b$	$(25, 5, 5)^T$ m
RIS element spacing	$d$	$\nu/f_d/2$
Number of RIS elements	$N$	100
Communication		
DC frequency	$f_d$	3 GHz
DC bandwidth	$B_d$	180 kHz
UE transmit power	$\rho_u, \rho_b$	24 dBm
UE/RIS noise power	$\sigma_u^2, \sigma_r^2$	-94 dBm
Paradigms		
Codebooks cardinality	$C_{CE}, C_{CB}^{\text{fix}}, C_{CB}^{\text{fle}}$	$N, \lceil N/3 \rceil, N$
Overall frame duration	$\tau$	[10, 200] ms
TTI duration	$T$	0.5 ms
Guard period	$\tau_s$	50 $\mu$ s
Pilot sequence length	$p$	1
OPT-CE processing in TTIs	$A$	5
Control packet content		
ID & Configuration bits	$b^{\text{ID}}, b^{\text{conf}}$	8
TTIs & Guard period bits	$b^{\text{frame}}, b^{\text{guard}}$	16
SE table bits	$b^{\text{SE}}$	6
RIS quantization level bits	$b^{\text{quant}}$	2

the length of the frame  $\tau$ , and the *set* of configuration  $C_{CB}$  to switch through, encoded in the (unsigned) integers  $b^{\text{frame}}$  and  $C_{CB}b^{\text{conf}}$ , respectively. Instead, the Setup contains different information. In particular, the payload of the SET-U is empty, according to the fixed rate transmission used by this paradigm. The payload of the SET-R contains the configuration  $c^*$  encoded by the same  $b^{\text{conf}}$  bits, representing an index in the common codebook. To summarize, the packet length is:

$$b_i^{(k)} = b^{\text{ID}} + 1 + \begin{cases} b^{\text{frame}} + b^{\text{guard}} + b^{\text{conf}}, & k = u, i = 1, \\ b^{\text{frame}} + C_{CB}b^{\text{conf}}, & k = r, i = 1, \\ 0, & k = u, i = 2, \\ b^{\text{conf}}, & k = r, i = 2. \end{cases} \quad (33)$$

Remark that the informative content of the CB-BSW packets is lower or equal to the one of OPT-CE, leading the former to be more reliable than the latter.

## V. NUMERICAL RESULTS AND DISCUSSION

This section presents the performance evaluation of the communication paradigms under consideration<sup>13</sup>. The parameters set for the simulations are given in Table 1, if not otherwise specified. The scenario is tested through Monte Carlo simulations. Concerning the scenario described in Section II,

<sup>13</sup>The simulation code for the paper is available at <https://github.com/lostinafro/ris-control>.

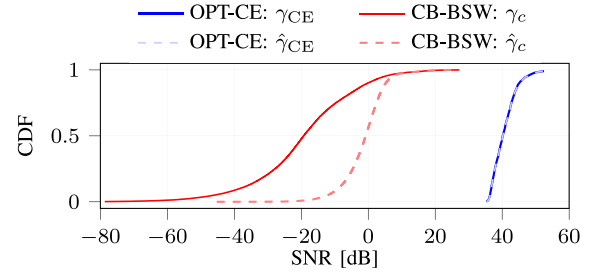


**FIGURE 5.** CDF of the actual ( $\gamma$ ) and estimated ( $\hat{\gamma}$ ) SNR on the DC for the communication paradigms under investigation.

we consider that the BS and RIS positions  $\mathbf{x}_b$  and  $\mathbf{x}_r = (0, 0, 0)^T$  are kept fixed, while the UE position,  $\mathbf{x}_u$ , changes at every simulation according to a uniform distribution with intervals  $(-D/2, 0, 0)^T$  and  $(D/2, D, -D)^T$ . When referring to average performance, we implicitly assume averaging over different UE positions and noise realizations. The channel coefficients of the DC are evaluated considering the LoS component of  $\mathbf{h}_d$  and  $\mathbf{g}_d$  following the model of [35, Section II]. Note that the RIS-OB-CC uses a different operating frequency and bandwidth w.r.t. the DC ones, while, for the IB-CC, we have  $f_r = f_d$  and  $B_r = 5B_d$ . The UE-CC has operating frequency  $f_u = f_d$  and bandwidth  $B_u = 5B_d$ . The overall frame duration  $\tau$  reflects the coherence time of the channel: a low  $\tau$  represents a high mobility environment with low coherence time, and vice versa. The TTI duration is set to half of the subframe duration in the orthogonal frequency-division multiplexing (OFDM) 5G NR standard [53]; carrier frequency, bandwidth, transmit and noise power follow the 5G NR standard [54]. The guard period is set to be 10% of the TTI as a reasonable value. For the OPT-CE paradigm, the channel estimation codebook  $C_{CE}$  is designed from the DFT, as described in Section III-B. For the sake of simplicity, the same configurations are used in the beam sweeping codebook  $C_{CB}$ . In particular, the codebook used by the CB-BSW with flexible frame structure is  $C_{CB}^{\text{fle}} = C_{CE}$ , while the one used by the CB-BSW with fixed frame structure uses one every three configurations, to take advantage of the possible lower overhead. Next, we divide the results into two parts: evaluating the paradigms performance under error-free CCs and investigating the impact of CCs reliability.

### A. PARADIGMS PERFORMANCE (ERROR-FREE CCs)

Fig. 5 depicts the CDF of the actual and estimated SNRs to give some insight into the impact of the possible algorithm errors. From the figure, it can be inferred that the noise impact on the SNR estimation is generally negligible for the OPT-CE paradigm. This finding is justified by the fact that the power of the noise influencing the measurement is proportional to  $1/C_{CE}$ , where  $C_{CE} \geq N$  (see Section III-B). On the other hand, when employing the CB-BSW paradigm, the SNR is measured per each configuration, and the resulting noise has a higher impact on the estimation.

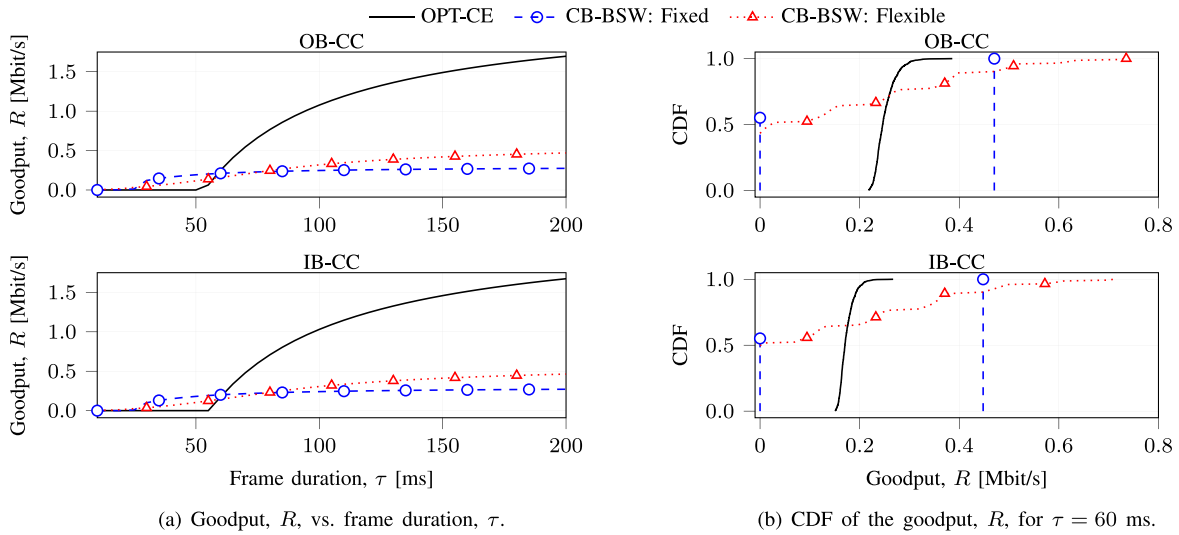


FIGURE 6. Analysis of the goodput performance.

Moreover, it can be observed that the SNR of the CB-BSW extends to very low values, while the minimum target KPI needs to be set to provide a non-negligible and supportable SE (at least higher than  $-13$  dB to reach the minimum SE value 0.0586 of 5G NR [54, Table V.1.3.1-3]). Therefore, whatever reasonable target KPI is chosen, it will produce a relatively high outage probability. In summary, the OPT-CE paradigm is inherently more robust to algorithmic errors than the CB-BSW one.

To provide a fair comparison between the paradigms, we evaluate the optimal target SNR  $\gamma_0^*$  used as relevant KPI for the CB-BSW paradigm that maximize the expected goodput  $R$ . Tab. 2 presents the results obtained numerically through exhaustive search for the different CCs and for various values of  $\tau$ . We note that the optimal  $\gamma_0$  depends on the frame structure chosen, while it does not depend on the kind of CC. Moreover, the duration  $\tau$  influences slightly the optimal  $\gamma_0$  in the flexible structure, being approximately 13.84 dB for  $\tau = 30$  ms and 12.37 dB for  $\tau \in \{60, 90\}$  ms for the flexible frame structure, while approximately 10.90 dB for any value of  $\tau$  for the fixed frame structure. We remark that the selection of the target KPI is also scenario-dependent; hence, this procedure should be performed during the deployment of the RIS.

Using the optimal target SNR, we now compare the performance of the two paradigms. Fig. 6(a) illustrates  $R$  as a function of the overall frame duration. Again, the impact of the kind of CC on  $R$  is negligible. The main advantage of the CB-BSW approach is the possibility of providing a non-null transmission rate even in the presence of a lower coherence block ( $< 60$  ms), while the OPT-CE needs a longer time horizon to obtain the CSI and perform the Payload phase ( $\geq 60$  ms). On the other hand, as long as the time horizon is sufficiently long ( $\tau \geq 75$  ms), the OPT-CE paradigm outperforms the CB-BSW one. In Fig. 6(b), we show the CDF of the goodput for  $\tau = 60$  ms. For this frame duration,

TABLE 2. Target SNR  $\gamma_0^*$  [dB] maximizing the goodput  $R(\gamma_0^*)$  [Kbit/s] for the CB-BSW paradigm for different CCs and frame duration  $\tau$ .

$\tau$ [ms]	CC	Fixed frame		Flexible frame	
		$\gamma_0^*$	$R(\gamma_0^*)$	$\gamma_0^*$	$R(\gamma_0^*)$
30	OB	10.90	52.1	13.84	29.7
	IB	10.90	26.1	13.84	23.7
60	OB	10.90	221.6	12.37	126.4
	IB	10.90	208.6	12.37	114.1
90	OB	10.90	278.1	12.37	246.9
	IB	10.90	269.4	12.37	234.0

the type of CC influences the performance of the OPT-CE paradigm, while it is less impactful on the CB-BSW performance. As expected, the IB-CC performs worse due to its increased overhead. Nevertheless, for the CB-BSW, approximately half of the transmissions have null goodput because of algorithmic errors, while the OPT-CE provide a non-null goodput for all values, corroborating the results of Fig. 5.

## B. IMPACT OF THE CCs RELIABILITY

Fig. 7 demonstrates the average utility (27) as a function of the probability of erroneous control  $1 - p_{cc}$ , for  $\tau = 60$  ms and both kinds of CC. The results of the transmission paradigms are in line with the ones presented in Fig. 6. The CC reliability influences significantly the performance when  $1 - p_{cc} \leq 0.05$ , i.e.,  $p_{cc} \geq 0.95$ . To consider a conservative case, we set a target reliability to be  $\bar{p}_{cc} = 0.99$ , and we study the minimum average SNRs  $\lambda_u$  and  $\lambda_r$  providing such reliability, following the control packet content given in Table 1. Fig. 8(a) shows the achieved  $p_{cc}$  for the OB-CC as a function of  $\lambda_u$  only, according to the assumption of error-free RIS-CC in the OB-CC case. With this kind of

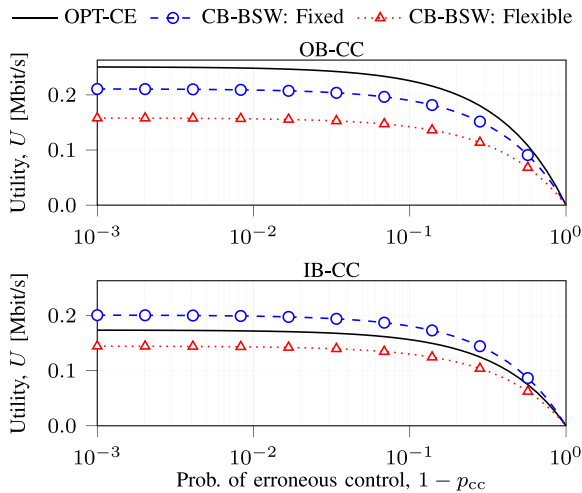


**FIGURE 7.** Analysis of the utility function,  $U$ , vs. probability of erroneous control,  $1 - p_{cc}$ , for  $\tau = 60$  ms.

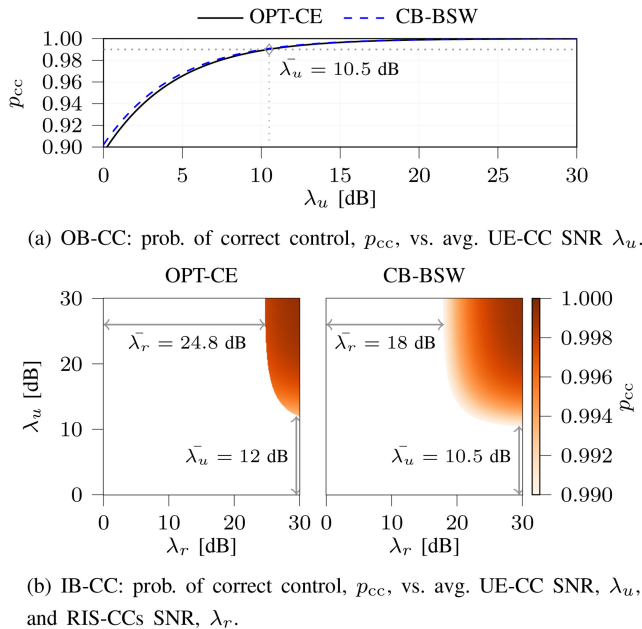


**FIGURE 8.** Impact of the CCs SNR on the reliability performance.

CC, the probabilities of correct control achieved by OPT-CE and CB-BSW have negligible differences, and  $\bar{\lambda}_u = 10.5$  dB is enough to provide the target correct control probability in both cases. Fig. 8(b) shows the  $p_{cc}$  as a heatmap function of  $\lambda_r$  and  $\lambda_u$  for the IB-CC case. Only the region satisfying the  $p_{cc} \geq 0.99$  is colored, and the minimum SNRs  $\bar{\lambda}_r$  and  $\bar{\lambda}_u$  needed are sketched. The OPT-CE needs higher SNRs than CB-BSW due to its control packets having higher information content. In particular, the need to transmit the phase-shift of each RIS element in the OPT-CE paradigm strongly impacts the overall reliability (see (32)). We remark that the performance provided by the CCs should be satisfied *simultaneously* to achieve the desired control reliability.

## VI. TOWARD MORE ELABORATED CONTROL DESIGNS

The presented systematic procedure paves the way for the control signaling design and quantification of more sophisticated RIS-empowered wireless systems. It can be applied, for example, to multi-user wideband/OFDM communications [1], [2], by accounting for the subcarrier allocation of the different control and payload messages. For this system setup, the Algorithmic phase needs to also consider the resource allocation process, whose output should be signaled to the UEs through a specific design of the Setup phase. In addition, the current framework, by omitting, merging, or repeating some of its general phases, can set the basis for the control design in RIS-assisted networks with a multi-antenna BS and multi-antenna UEs, and smart wireless environments with multiple, possibly machine learning orchestrated, RISs [55], as well as shared RISs among multiple communications pairs [4]. Of late interest are also multi-functional RISs [8], and especially those possessing sensing capabilities [15], which may provide higher flexibility for efficient control signaling designs [36].

We next elaborate in more detail on the case where the BS is equipped with multiple antennas and there exists the possibility of a weak direct link between itself and the UE. For the OPT-CE communication paradigm, the RIS configuration and the BS combiner can be jointly optimized [2], [18], [56], at the cost of a longer Algorithmic phase, i.e., higher CE and computation overhead and complexity. It is noted, however, that the increased beamforming gain from the multiple BS antennas might lead to cases where the BS-UE link is satisfactory, implying that the RIS deployment can be avoided, reducing the control overhead. For this mode to be realized, the operation protocol needs to enable, for example, the separate estimation of the UE-RIS-BS and UE-BS channels, via activation/deactivation of the RIS panel, as well as a relevant action during the Initialization phase. There exist various modes of operation when the CB-BSW paradigm is adopted. One is to perform BSW at the BS during the Initialization phase, together with BSW at the RIS, again at a cost of a larger overhead for both the fixed and flexible frame structures. Alternatively, to reduce the control signaling overhead, the BS combiner can be designed to solely match its channel with the RIS, or that with the UE if the aid of the RIS results to be negligible. One way to achieve the former is to capitalize on the common assumption that the RIS is placed such that there exists a strong line-of-sight with the BS [5]. In this way, the BS may adopt the reception configuration closest to maximal ratio combining. When the RIS can be avoided, the BS combiner can be similarly designed, now for the channel towards the UE - this operational mode can be decided similarly to the respective OPT-CE case.

It is finally noted that OPT-CE and CB-BSW can be combined to devise additional signaling schemes. One example is presented in [22], where the CB-BSW is performed to set the RIS configuration when the link budget falls below a certain threshold, and then OPT-CE follows to set the BS

combiner and/or the UE beamformer, treating the configured RIS as an unknown scatterer.

## VII. CONCLUSION

In this paper, we proposed a systematic procedure consisting of four phases (Initialization, Algorithmic, Setup, and Payload) to evaluate RIS-enabled communication performance while addressing the impact of control and signaling procedures. The data exchange and the frame structure for two different communication paradigms, namely OPT-CE and CB-BSW, were detailed. The performance of the paradigms was analyzed employing a utility function that considers the overhead generated by its various phases, the possible errors coming from the Algorithmic phase, and the impact of losing control packets needed for signaling purposes. Moreover, we particularized the performance evaluation for two kinds of CCs connecting the decision maker and the RISC (IB-CC and OB-CC), showcasing the minimum performance needed to obtain the desired control reliability. Our extensive performance evaluation results showcased that CB-BSW is better suited for high mobility scenarios, since its operation is not reliant on having full channel knowledge that needs to be obtained within a given coherence time. Furthermore, OPT-CE requires exchanging more control data necessitating higher coding rate, and thus, higher SNR. For that reason, OPT-CE visibly benefits from using OB-CC rather than IB-CC. On the other hand, when the channel coherence time is sufficiently long and high SNR can be ensured on the CCs, OPT-CE can offer much higher throughput. It is also inherently more robust to algorithmic errors than CB-BSW. Possible extensions of the proposed procedure for more sophisticated scenarios of interest were discussed. Together with those extensions, in the future, we intend to study the impact of synchronization errors on the frame level and in the PHY-layer resources.

## REFERENCES

- [1] C. Huang et al., "Reconfigurable intelligent surfaces for energy efficiency in wireless communication," *IEEE Trans. Wireless Commun.*, vol. 18, no. 8, pp. 4157–4170, Aug. 2019.
- [2] Q. Wu, S. Zhang, B. Zheng, C. You, and R. Zhang, "Intelligent reflecting surface aided wireless communications: A tutorial," *IEEE Trans. Commun.*, vol. 69, no. 5, pp. 3313–3351, May 2021.
- [3] E. Calvanese Strinati et al., "Reconfigurable, intelligent, and sustainable wireless environments for 6G smart connectivity," *IEEE Commun. Mag.*, vol. 59, no. 10, pp. 99–105, Oct. 2021.
- [4] G. C. Alexandropoulos et al., "RIS-enabled smart wireless environments: Deployment scenarios, network architecture, bandwidth and area of influence," *EURASIP J. Wireless Commun. Netw.*, vol. 2023, Oct. 2023, Art. no. 103.
- [5] G. C. Alexandropoulos, K. D. Katsanos, M. Wen, and D. B. Da Costa, "Counteracting eavesdropper attacks through reconfigurable intelligent surfaces: A new threat model and secrecy rate optimization," *IEEE Open J. Commun. Soc.*, vol. 4, pp. 1285–1302, 2023.
- [6] N. Awarkeh, D.-T. Phan-Huy, and R. Visoz, "Electro-magnetic field (EMF) aware beamforming assisted by reconfigurable intelligent surfaces," in *Proc. IEEE 22rd Int. Workshop Signal Process. Adv. Wireless Commun. (SPAWC)*, Lucca, Italy, 2021, pp. 541–545.
- [7] E. Björnson, H. Wymeersch, B. Matthiesen, P. Popovski, L. Sanguinetti, and E. de Carvalho, "Reconfigurable intelligent surfaces: A signal processing perspective with wireless applications," *IEEE Signal Process. Mag.*, vol. 39, no. 2, pp. 135–158, Mar. 2022.
- [8] M. Jian et al., "Reconfigurable intelligent surfaces for wireless communications: Overview of hardware designs, channel models, and estimation techniques," *Intell. Conver. Netw.*, vol. 3, no. 1, pp. 1–32, 2022.
- [9] R. A. Tasci, F. Kilinc, E. Basar, and G. C. Alexandropoulos, "A new RIS architecture with a single power amplifier: Energy efficiency and error performance analysis," *IEEE Access*, vol. 10, pp. 44804–44815, 2022.
- [10] R. Faqiri, C. Saigre-Tardif, G. C. Alexandropoulos, N. Shlezinger, M. F. Imani, and P. del Hougne, "PhysFad: Physics-based end-to-end channel modeling of RIS-parametrized environments with adjustable fading," *IEEE Trans. Wireless Commun.*, vol. 22, no. 1, pp. 580–595, Jan. 2023.
- [11] Z. Wang, L. Liu, and S. Cui, "Channel estimation for intelligent reflecting surface assisted multiuser communications: Framework, algorithms, and analysis," *IEEE Trans. Wireless Commun.*, vol. 19, no. 10, pp. 6607–6620, Oct. 2020.
- [12] A. L. Swindlehurst, G. Zhou, R. Liu, C. Pan, and M. Li, "Channel estimation with reconfigurable intelligent surfaces—A general framework," *Proc. IEEE*, vol. 10, no. 9, pp. 1312–1338, Sep. 2022.
- [13] L. Mo, F. Saggese, X. Lu, Z. Wang, and P. Popovski, "Direct tensor-based estimation of broadband mmWave channels with RIS," *IEEE Commun. Lett.*, vol. 27, no. 7, pp. 1849–1853, Jul. 2023.
- [14] H. Zhang et al., "Channel estimation with hybrid reconfigurable intelligent metasurfaces," *IEEE Trans. Commun.*, vol. 71, no. 4, pp. 2441–2456, Apr. 2023.
- [15] G. C. Alexandropoulos, N. Shlezinger, I. Alamzadeh, M. F. Imani, H. Zhang, and Y. C. Eldar, "Hybrid reconfigurable intelligent metasurfaces: Enabling simultaneous tunable reflections and sensing for 6G wireless communications," *IEEE Veh. Technol. Mag.*, vol. 19, no. 1, pp. 75–84, Mar. 2024.
- [16] V. Popov et al., "Experimental demonstration of a mmWave passive access point extender based on a binary reconfigurable intelligent surface," *Front. Commun. Netw.*, vol. 2, Oct. 2021, Art. no. 733891.
- [17] Q. Wu and R. Zhang, "Intelligent reflecting surface enhanced wireless network via joint active and passive beamforming," *IEEE Trans. Wireless Commun.*, vol. 18, no. 11, pp. 5394–5409, Nov. 2019.
- [18] P. Mursia, V. Sciancalepore, A. Garcia-Saavedra, L. Cottatellucci, X. C. Pérez, and D. Gesbert, "RISMA: Reconfigurable intelligent surfaces enabling beamforming for IoT massive access," *IEEE J. Sel. Areas Commun.*, vol. 39, no. 4, pp. 1072–1085, Apr. 2021.
- [19] M. Yue, L. Liu, and X. Yuan, "RIS-aided multiuser MIMO-OFDM with linear precoding and iterative detection: Analysis and optimization," *IEEE Trans. Wireless Commun.*, vol. 22, no. 11, pp. 7606–7619, Nov. 2023.
- [20] J. An et al., "Codebook-based solutions for reconfigurable intelligent surfaces and their open challenges," *IEEE Wireless Commun.*, vol. 31, no. 2, pp. 134–141, Apr. 2024.
- [21] C. Singh, K. Singh, and K. H. Liu, "Fast beam training for RIS-assisted uplink communication," 2021, [arXiv:2107.14138](https://arxiv.org/abs/2107.14138).
- [22] V. Jamali, G. C. Alexandropoulos, R. Schober, and H. V. Poor, "Low-to-zero-overhead IRS reconfiguration: Decoupling illumination and channel estimation," *IEEE Commun. Lett.*, vol. 16, no. 4, pp. 932–936, Apr. 2022.
- [23] G. C. Alexandropoulos, V. Jamali, R. Schober, and H. V. Poor, "Near-field hierarchical beam management for RIS-enabled millimeter wave multi-antenna systems," in *Proc. IEEE 12th Sensor Array Multichannel Signal Process. Workshop (SAM)*, 2022, pp. 460–464.
- [24] M. Rahal et al., "Performance of RIS-aided nearfield localization under beams approximation from real hardware characterization," *EURASIP J. Wireless Commun. Netw.*, vol. 2023, Aug. 2023, Art. no. 86.
- [25] J. Wang, W. Tang, S. Jin, C.-K. Wen, X. Li, and X. Hou, "Hierarchical codebook-based beam training for RIS-assisted mmWave communication systems," *IEEE Trans. Commun.*, vol. 71, no. 6, pp. 3650–3662, Jun. 2023.
- [26] X. Cao et al., "Massive access of static and mobile users via reconfigurable intelligent surfaces: Protocol design and performance analysis," *IEEE J. Sel. Areas Commun.*, vol. 40, no. 4, pp. 1253–1269, Apr. 2022.
- [27] V. Croisfelt, F. Saggese, I. Leyva-Mayorga, R. Kotaba, G. Gradoni, and P. Popovski, "A random access protocol for RIS-aided wireless communications," in *Proc. IEEE 23rd Int. Workshop Signal Process. Adv. Wireless Commun. (SPAWC)*, Oulu, Finland, 2022, pp. 1–5.



- [28] V. Croisfelt, F. Saggese, I. Leyva-Mayorga, R. Kotaba, G. Gradoni, and P. Popovski, "Random access protocol with channel oracle enabled by a reconfigurable intelligent surface," *IEEE Trans. Wireless Commun.*, vol. 22, no. 12, pp. 9157–9171, Dec. 2023.
- [29] X. Cao, B. Yang, H. Zhang, C. Huang, C. Yuen, and Z. Han, "Reconfigurable-intelligent-surface-assisted MAC for wireless networks: Protocol design, analysis, and optimization," *IEEE Internet Things J.*, vol. 8, no. 18, pp. 14171–14186, Sep. 2021.
- [30] Z. Zhang, S. Atapattu, Y. Wang, and M. Di Renzo, "Distributed CSMA/CA MAC protocol for RIS-assisted networks," in *Proc. IEEE Global Commun. Conf. (GLOBECOM)*, 2023, pp. 2402–2407.
- [31] S. Hao and H. Zhang, "Performance analysis of PHY layer for RIS-assisted wireless communication systems with retransmission protocols," *J. Comp. Inf. Sci.*, vol. 34, no. 8, pp. 5388–5404, 2022.
- [32] M. Di Renzo et al. "Smart radio environments empowered by reconfigurable intelligent surfaces: How it works, state of research, and the road ahead," *IEEE J. Sel. Areas Commun.*, vol. 38, no. 11, pp. 2450–2525, Nov. 2020.
- [33] B. Zheng and R. Zhang, "Intelligent reflecting surface-enhanced OFDM: Channel estimation and reflection optimization," *IEEE Wireless Commun.*, vol. 9, no. 4, pp. 518–522, Apr. 2020.
- [34] L. Subrt and P. Pechac, "Controlling propagation environments using intelligent walls," in *Proc. 6th Eur. Conf. Antennas Propag. (EUCAP)*, 2012, pp. 1–5.
- [35] A. Albanese, F. Devoti, V. Sciancalepore, M. Di Renzo, and X. Costa-Pérez, "MARISA: A self-configuring metasurfaces absorption and reflection solution towards 6G," in *Proc. IEEE INFOCOM*, 2022, pp. 250–259.
- [36] V. Croisfelt, F. Devoti, F. Saggese, V. Sciancalepore, X. Costa-Pérez, and P. Popovski, "An orchestration framework for open system models of reconfigurable intelligent surfaces," 2023, *arXiv:2304.10858*.
- [37] O. Tsilipakos et al., "Toward intelligent metasurfaces: The progress from globally tunable metasurfaces to software-defined metasurfaces with an embedded network of controllers," *Adv. Opt. Mater.*, vol. 8, no. 17, 2020, Art. no. 2000783.
- [38] C. Liaskos et al., "Integrating software-defined metasurfaces into wireless communication systems: Design and prototype evaluation," in *Proc. IEEE Symp. Comput. Commun. (ISCC)*, 2022, pp. 1–6.
- [39] C. Liaskos et al., "Software-defined reconfigurable intelligent surfaces: From theory to end-to-end implementation," *Proc. IEEE*, vol. 110, no. 9, pp. 1466–1493, Sep. 2022.
- [40] A. Zappone, M. Di Renzo, F. Shams, X. Qian, and M. Debbah, "Overhead-aware design of reconfigurable intelligent surfaces in smart radio environments," *IEEE Trans. Wireless Commun.*, vol. 20, no. 1, pp. 126–141, Jan. 2021.
- [41] A. Jalili, H. Nazari, S. Namvarasl, and M. Keshtgari, "A comprehensive analysis on control plane deployment in SDN: In-band versus out-of-band solutions," in *Proc. IEEE 4th Int. Conf. Knowl.-Based Eng. Innov. (KBEI)*, 2017, pp. 1025–1031.
- [42] D. Lopez-Pajares, J. Alvarez-Horcajo, E. Rojas, A. S. M. Asadujjaman, and I. Martinez-Yelmo, "Amaru: Plug&play resilient in-band control for SDN," *IEEE Access*, vol. 7, pp. 123202–123218, 2019.
- [43] X. Dong et al., "Joint controller placement and control-service connection in hybrid-band control," *IEEE Trans. Cloud Comp.*, vol. 11, no. 3, pp. 3139–3152, Jul./Sep. 2023.
- [44] B. F. Lo, "A survey of common control channel design in cognitive radio networks," *Phys. Commun.*, vol. 4, no. 1, pp. 26–39, 2011.
- [45] P. Popovski, *Wireless Connectivity: An Intuitive and Fundamental Guide*, vol. 3. Hoboken, NJ, USA: Wiley, 2020.
- [46] M. He, W. Xu, and C. Zhao, "RIS-assisted broad coverage for mmWave massive MIMO system," in *Proc. IEEE ICC*, 2021, pp. 1–6.
- [47] P. Ramezani, M. A. Gimyk, and E. Bjornson, "Broad beam reflection for RIS-assisted MIMO systems with planar arrays," in *Proc. 57th Asilomar Conf. Signals, Syst., Comput.*, 2023, pp. 504–508.
- [48] T. Yucek and H. Arslan, "MMSE noise power and SNR estimation for OFDM systems," in *Proc. IEEE Sarnoff Symp.*, 2006, pp. 1–4.
- [49] E. Björnson, J. Hoydis, and L. Sanguinetti, "Massive MIMO networks: Spectral, energy, and hardware efficiency," *Found. Trends Signal Process.*, vol. 11, nos. 3–4, pp. 154–655, 2017.
- [50] S. M. Kay, *Fundamentals of Statistical Signal Processing: Estimation Theory*. Hoboken, NY, USA: Prentice-Hall, 1997.
- [51] C. Shannon, "Communication in the presence of noise," *Proc. IRE*, vol. 37, no. 1, pp. 10–21, 1949.
- [52] D. Selimis, K. P. Peppas, G. C. Alexandropoulos, and F. I. Lazarakis, "On the performance analysis of RIS-empowered communications over Nakagami- $m$  fading," *IEEE Commun. Lett.*, vol. 25, no. 7, pp. 2191–2195, Jul. 2021.
- [53] "Study on new radio (NR) access technology, version 15.0.0," 3GPP, Sophia Antipolis, France, Rep. 21.915, 2019.
- [54] "NR; physical layer procedures for data, version 15.0.0," 3GPP, Sophia Antipolis, France, Rep. 38.214, 2022.
- [55] G. C. Alexandropoulos, K. Stylianopoulos, C. Huang, C. Yuen, M. Bennis, and M. Debbah, "Pervasive machine learning for smart radio environments enabled by reconfigurable intelligent surfaces," *Proc. IEEE*, vol. 110, no. 9, pp. 1494–1525, Sep. 2022.
- [56] F. Saggese et al., "Control aspects for using RIS in latency-constrained mobile edge computing," in *Proc. 57th Asilomar Conf. Signals, Syst., Comput.*, 2023, pp. 174–181.